

Investigation of solvent effect on photophysical properties of some sulfonamides derivatives

Ebru BOZKURT^{1,*}, Halise İnci GÜL², Mehtap TUĞRAK²

¹Program of Occupational Health and Safety, Erzurum Vocational Training School, Atatürk University, Erzurum, Turkey

²Department of Pharmaceutical Chemistry, Faculty of Pharmacy, Atatürk University, Erzurum, Turkey

Received: 21.04.2016

Accepted/Published Online: 13.10.2016

Final Version: 19.04.2017

Abstract: The photophysical properties of new sulfonamides synthesized recently were investigated in different solvents. Shifts in the absorption and fluorescence spectra of both compounds (S10 and S11) occurred depending on the solvents used. Ground and excited state dipole moments of the molecules were calculated using the spectral shifts of the compounds in different solvents and polarity function of solvents, respectively. They were 1.32 and 1.46 D for S10 and 1.71 and 4.89 D for S11. These results suggested that the excited state dipole moments are greater than those in ground state for both molecules. This means that the dyes were more polar in excited state compared with ground state. It was concluded that the changes in the dipole moments arise from both solvent–solute interaction and solvent polarity.

Key words: Sulfonamide, absorption, fluorescence, solvent polarity, Stokes shift

1. Introduction

Solvent effect plays an important role in the photophysical properties of organic molecules.^{1–4} The changes in photophysical parameters and spectral shifts arise from specific or nonspecific solvent–solute interactions.^{5–7} The nature of the microenvironment around the solute molecules is very effective on electronic transitions in the molecules. The solvent–solute interactions at the microscopic level can be discussed using polarity scale or solvatochromic parameters. The ground and excited state dipole moments of solute molecules change with the solvent effect. Determination of the dipole moment of the molecule provides information about the geometric and electronic structure of the molecule.^{8–11} This information sheds light on many areas such as designing nonlinear optical materials using fluorescence probes and biophysical studies about the polarity of the microenvironment lipid bilayers, proteins, and peptides.^{12–14}

The synthesis of novel π -conjugated organic compounds is a very important area due to their wide applications in various fields such as optoelectronics, bio-imaging, and optical storage devices during the last few decades.^{15–17} These molecules exhibit interesting optical and spectral properties since they have both electron donating (D) and accepting (A) substituents in a single molecule and intramolecular charge transfer (ICT).¹⁸ Therefore, they contribute to research in areas such as nonlinear optical devices, chemical sensing,^{19,20} and understanding photochemical.²¹ and photobiological processes. Changes in the spectral properties of these compounds depending on the solvent polarity would allow the creation of favorable conditions in the area to be used.²²

*Correspondence: ebrubozkurt@atauni.edu.tr

The present study investigated the spectral behaviors of the new sulfonamide derivatives compound S10 [4-(2-(2,3-dihydro-1H-inden-1-ylidene) hydrazine) benzenesulfonamide] and compound S11 [4-(2-(1,3-dihydro-2H-inden-2-ylidene)hydrazino) benzenesulfonamide] in different solvents. For this purpose, it was planned to take UV-Vis absorption, steady-state, and time-resolved fluorescence measurements for the S10 and S11 molecules in different solvents to investigate the solvent–solute interactions to calculate the ground and excited state dipole moments of these new compounds. Biochemical research such as biosensing will shed light on determining the effect of the environment on the spectral properties of these biologically active compounds.

2. Results and discussion

The 4-(2-substituted hydrazinyl)benzenesulfonamide derivatives (S10–S11) were synthesized. These compounds were evaluated for their hCA I and II isoenzymes and found to be sufficiently active in our previous study.²³ In the present study, the absorption and fluorescence measurements of compounds S10 and S11 were realized in various solvents with different polarity at room temperature (Figures 1a and 1b and 2a and 2b). As can be seen in the absorption spectra, while the absorption spectrum of S10 consists of one band in the 340 nm region, S11 has two bands at 380 nm and a shorter-wavelength band near 299 nm. The fluorescence emission spectra of S10 and S11 were recorded at excitation wavelength 320 nm. As shown in Figures 2a and 2b, the structure of the fluorescence spectra of S10 did not change with solvent but the fluorescence spectra of S11 displayed structural differences depending on solvent. The exhibition of distinct spectral characteristics of these two compounds having similar skeletons was a very interesting result. It appears that the position of the indanone group causes a considerable change in π electron mobility (Scheme 1). As can be seen in Scheme 1, while compound S11 presents only one charge transfer state (Type B), compound S10 presents two different charge transfer states (Types A and B). This suggested that the two compounds should possess different photophysical characters. When the fluorescence spectra of S11 were taken, some shoulders between 400 and 500 nm were observed (Figure 2b). To explain this situation, i.e. the shoulders between 400 and 500 nm, excitation spectra were also taken. Differences between excitation and absorption spectra showed that the structure of the excimer did not form for S11.

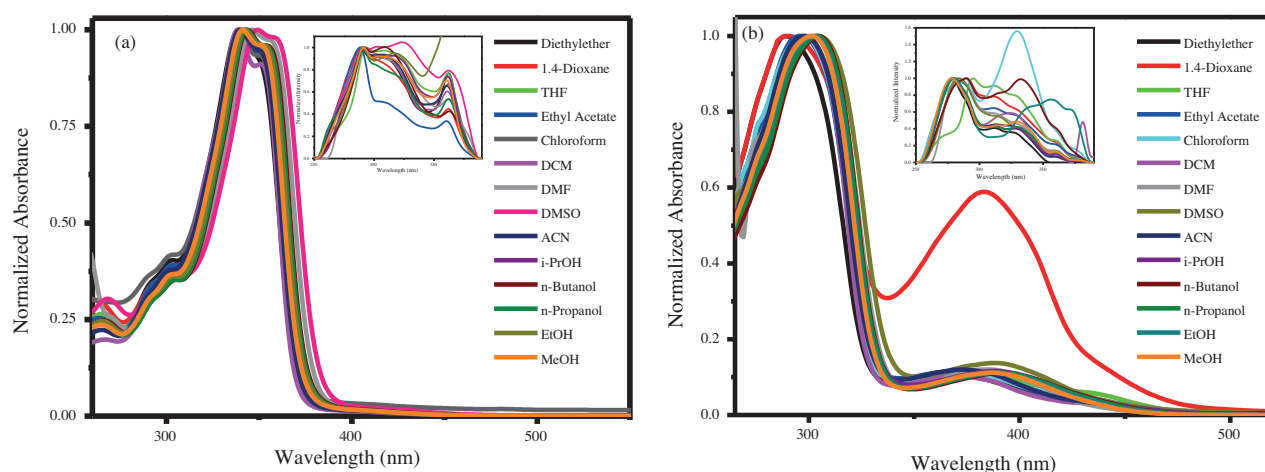
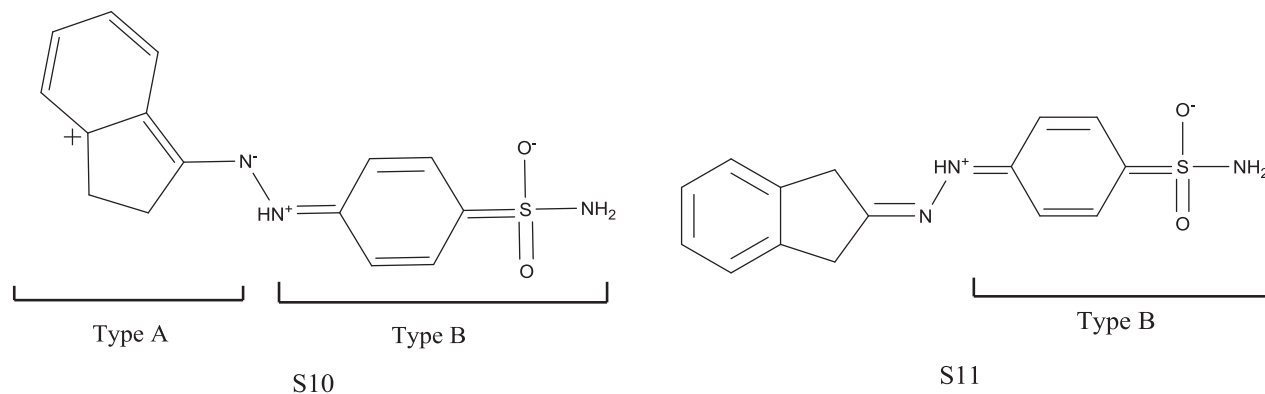


Figure 1. Normalized absorption spectra of (a) S10 (b) S11 in different solvents. Insets: Normalized excitation spectra.

Changes in the fluorescence peak positions were observed depending on solvent polarity. As shown in Table 1, the shifts in the absorption and fluorescence spectra observed depend on solvent polarity. The changes

in both absorption and fluorescence spectra proved the effects on the ground and excited states of molecules resulting from polarity or hydrogen bond interactions between the solvent molecules and the sulfonamide derivatives.²⁴ The Stokes shifts observed in nonpolar solvents were greater than in the polar solvent. This suggested that dipole-dipole interactions were stronger than the hydrogen bond interactions.



Scheme 1. Possible resonance structure of compounds.

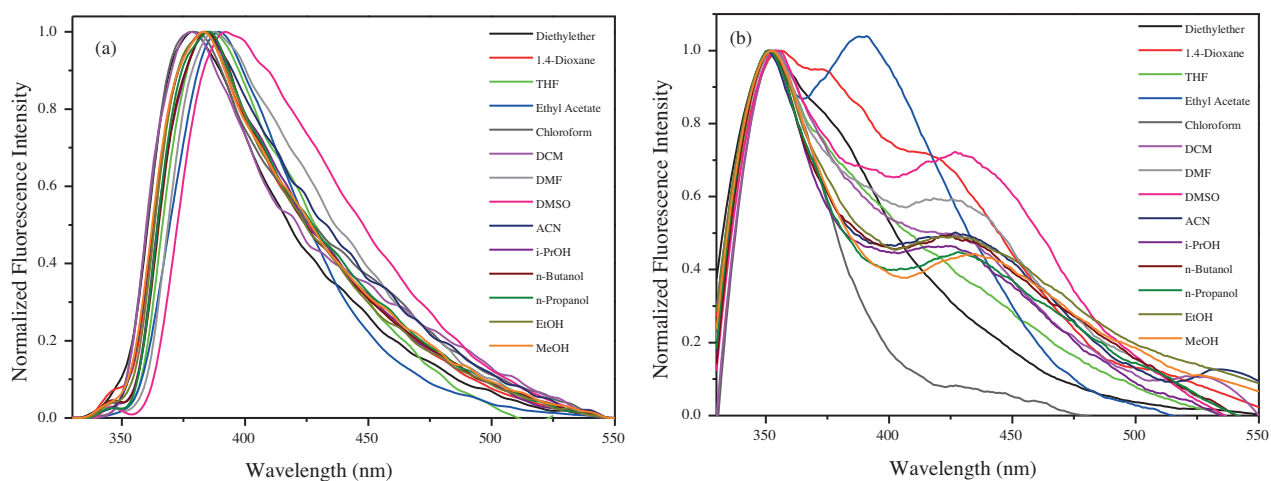


Figure 2. Normalized fluorescence spectra of (a) S10 (b) S11 in different solvents ($\lambda_{exc} = 320$ nm).

It was determined that fluorescence quantum yield, fluorescence lifetime, and radiative and nonradiative rate constants of the compounds change depending on the solvent used. Figures 3a and 3b show fluorescence decay curves of S10 and S11 in different solvents. Generally, quantum yield (Φ_f) and lifetime (τ_f) values in other solvents were higher compared to polar protic solvents (Table 2). This may be due to the fact that fluorophores are quenched by polar solvents due to hydrogen bonds.²⁵ Both Φ_f and τ_f values did not show a significant change in polar solvents depending on solvent polarity. Furthermore, high k_{nr} values of compounds in polar solvents show that the main path of the excited state deactivation is internal conversion.⁸ Herein, the increase in k_{nr} in polar solvents can be associated with twisted intramolecular charge transfer (TICT) state.^{26,27} Furthermore, hydrogen bond interactions, which cause intramolecular proton transfer from the solvent to molecule, may contribute to radiative transitions.²⁸ It was indicated that the fluorescence quantum yield of S11 is very low compared to S10 in all the solvents. S10 was more fluorescent than S11 due to differences in the binding position of the indanone group to the hydrazine moiety, which affect the electronic structures

of the molecules. Moreover, it was observed that the quantum yield of S10 is very low in ACN despite having an aprotic nature. This could be explained by an increased twisting of the single bonds involved in the charge transfer in the excited state for ACN.²⁹

Table 1. Absorption and fluorescence spectral data of S10 and S11 in different solvents ($\lambda_{exc} = 320$ nm).

Solvent	λ_{abs} (nm)	λ_{fluor} (nm)	$\nu_a - \nu_f$ (cm ⁻¹)	$\nu_a + \nu_f$ (cm ⁻¹)
S10				
Diethylether	339	379	3113	55,884
1.4-Dioxane	341	384	3284	55,367
Chloroform	339	381	3252	55,745
DCM	338	381	3339	55,833
THF	343	388	3381	54,928
Ethyl acetate	340	390	3771	55,053
DMF	346	386	2995	54,808
DMSO	349	391	3078	54,229
ACN	340	384	3370	55,453
i-PrOH	343	385	3180	55,129
n-Butanol	344	385	3096	55,044
n-PrOH	343	385	3180	55,129
EtOH	342	383	3130	55,349
MeOH	341	382	3148	55,504
S11				
Diethylether	289	348	5866	63,338
1.4-Dioxane	290	349	5829	63,136
Chloroform	298	355	5388	61,726
DCM	298	362	5933	61,181
THF	297	349	5017	62,323
Ethyl acetate	296	393	8338	59,229
DMF	300	349	4680	61,987
DMSO	304	348	4159	61,630
ACN	298	346	4655	62,459
i-PrOH	303	349	4350	61,657
n-Butanol	305	348	4051	61,523
n-PrOH	304	348	4159	61,630
EtOH	302	348	4377	61,848
MeOH	301	350	4651	61,794

The ground and excited state dipole moments of S10 and S11 were calculated. For this purpose, the slopes of plots of Stokes shifts versus polarity functions were determined using Eqs. (4) and (5) (Figures 4a and 4b). The ground (μ_g) and excited state dipole moments (μ_e) were calculated using Eqs. (11) and (12) and they were summarized in Table 3. The calculated dipole moments indicate that the excited state dipole moments were greater than those in ground state for both compounds. This increase in the excited state dipole moments demonstrated that the compounds are more polar in excited state as compared with ground state.^{11,24,30} However, the difference in the dipole moment clearly showed that the excited state S_1 will be energetically more stabilized relative to the ground state S_0 .¹⁴

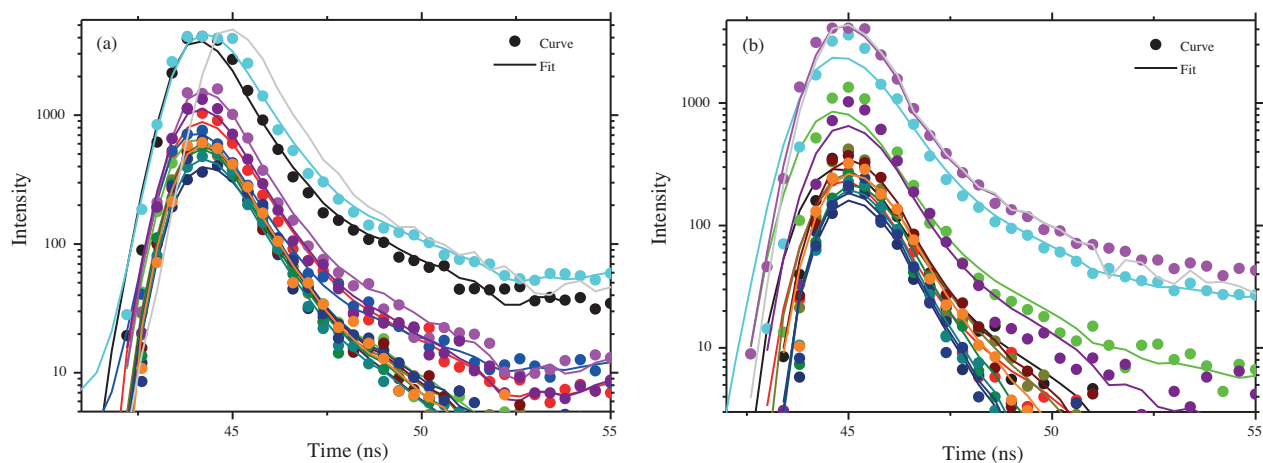


Figure 3. Fluorescence decay curves of (a) S10 and (b) S11 in •Diethylether; •1,4-dioxane; •THF; •Ethyl Acetate; •Chloroform; •DCM; •DMF; •DMSO; •ACN; •Isopropanol; •1-butanol; •1-propanol; •Ethanol; •Methanol; —IRF (Instrument Response Function).

Table 2. The photophysical parameters of S10 and S11 in different solvents.

Solvent	Φ_f	τ_f (ns)	$k_r \times 10^{-9}$ (s $^{-1}$)	$k_{nr} \times 10^{-9}$ (s $^{-1}$)
S10				
Diethylether	0.14	0.2057	0.6597	4.2017
1.4-Dioxane	0.38	0.4193	0.9132	1.4717
Chloroform	0.26	0.3874	0.6620	1.9193
DCM	0.15	0.2118	0.6998	4.0217
THF	0.16	0.2641	0.6027	3.1838
Ethyl acetate	0.33	0.6214	0.5332	1.0761
DMF	0.33	0.1903	1.7407	3.5142
DMSO	0.47	0.5032	0.9275	1.0598
ACN	0.16	0.2707	0.5881	3.1060
i-PrOH	0.19	0.2850	0.6582	2.8506
n-Butanol	0.22	0.2366	0.9201	3.3065
n-PrOH	0.21	0.2911	0.7062	2.7291
EtOH	0.19	0.2622	0.7262	3.0876
MeOH	0.16	0.2604	0.6118	3.2285
S11				
Diethylether	0.13	0.4115	0.3120	2.1181
1.4-Dioxane	0.11	0.2231	0.4740	4.0083
Chloroform	0.06	0.4570	0.1220	2.0662
DCM	0.13	0.4359	0.2921	2.0020
THF	0.09	0.3732	0.2417	2.4378
Ethyl acetate	0.12	0.2462	0.4903	3.5715
DMF	0.09	0.2654	0.3316	3.4363
DMSO	0.10	0.2374	0.4398	3.7725
ACN	0.09	0.1924	0.4903	4.7072
i-PrOH	0.06	0.1192	0.5008	7.8884
n-Butanol	0.06	0.1255	0.4968	7.4713
n-PrOH	0.06	0.0871	0.7132	10.7731
EtOH	0.08	0.1338	0.5816	6.8922
MeOH	0.08	0.0448	1.6777	20.6637

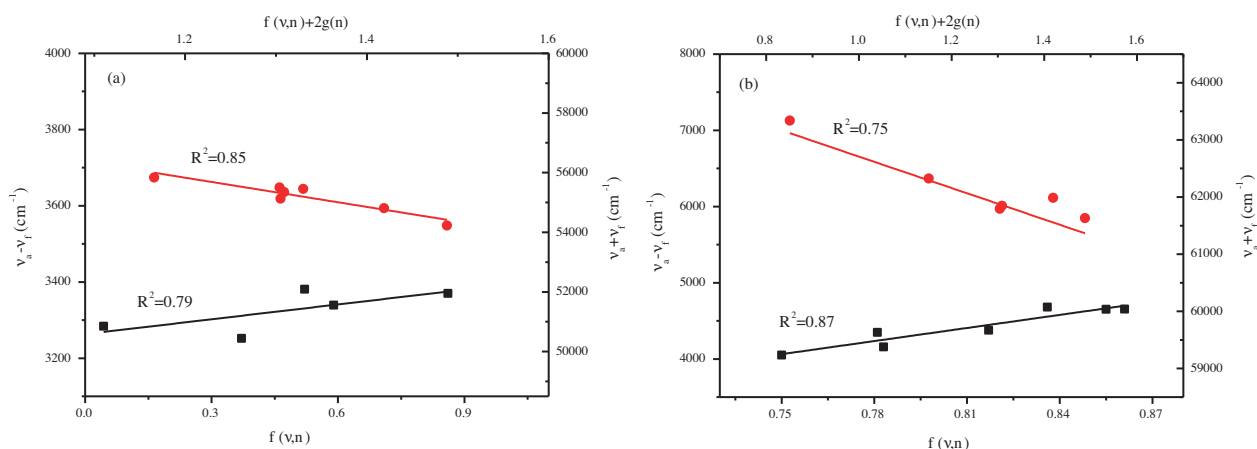


Figure 4. The plot of Stokes shift with $f(\varepsilon, n)$ (■) and $f(\varepsilon, n) + 2g(n)$ (●) for (a) S10, (b) S11.

Table 3. Calculated values of ground-state and excited-state dipole moments for S10 and S11.

Compound	μ_g^a (D)	μ_e^b (D)	$\Delta\mu^c$ (D)	$\Delta\mu^d$ (D)
S10	1.32	1.46	0.14	1.03
S11	1.71	4.89	3.18	2.95

^a The experimental ground-state dipole moments calculated by Eq. (11) ^b The experimental excited-state dipole moments calculated by Eq. (12) ^c The change in dipole moments for μ_e and μ_g ^d The change in dipole moments calculated by Eq. (14).

Additionally, the changes in dipole moments ($\Delta\mu$) were determined using molecular-microscopic solvent polarity parameter and Stokes shift (Figure 5). $\Delta\mu$ values, calculated using Eq. (14), are given in Table 3. To explain the changes in dipole moments, the relation between Stokes shifts and the solvent polarity parameter was used. If the changes in dipole moments were dependent on only solvent polarity, the plot of Stokes shifts versus solvent polarity parameter should have exhibited a linear trend. The empirical polarity scale developed by Reichardt $E_T(30)$ values has been used and Stokes shifts were plotted versus the solvent polarity parameter.³¹ According to Figures 6a and 6b, the plot of Stokes shift vs. $E_T(30)$ did not indicate a linear relationship. This proved that the changes in dipole moments arise from both solvent polarity and solvent-solute interactions.⁹

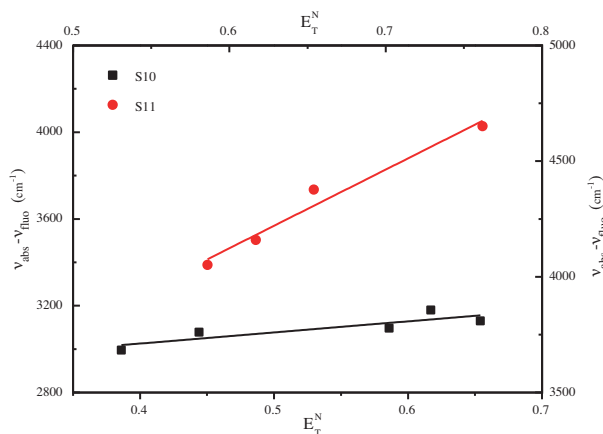


Figure 5. The plot of Stokes shift with molecular-microscopic solvent polarity parameter for (■) S10, (●) S11.

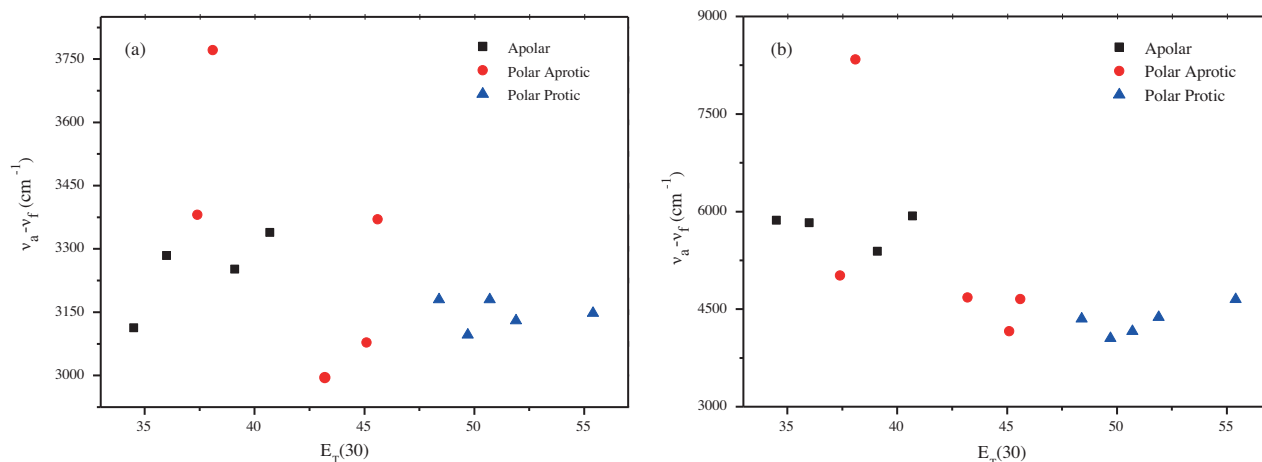


Figure 6. The variation in Stokes shift with $E_T(30)$ for (a) S10, (b) S11.

Table 4. Values of regression and correlation (r) coefficients obtained from MLR analysis.

	S10					S11				
	ν_0	a	b	c	r	ν_0	a	b	c	r
ν_{abs}	29,980.10	231.00	-892.40	-524.34	0.92	35,870.01	-575.37	-1189.32	-2721.81	0.93
ν_{em}	27,226.25	584.52	-1235.50	-1333.35	0.94	28,167.37	-466.13	1320.03	-222.52	0.78
$\Delta\nu$	2753.78	-352.50	341.34	809.41	0.98	7701.91	-109.66	-2508.67	-2498.64	0.94

The electron densities of the molecules change in the ground and excited states. Therefore, the dipole moments of S10 and S11 are different in these states mentioned above. The dipole moments for both compounds increase when they are excited. This suggests the existence of intramolecular charge transfer (ICT) and twisted intramolecular charge transfer (TICT) in excited state. The possible resonance structures of these compounds are shown in Scheme 1. TICT state occurs for S10 due to the possibility of Type A resonance as shown in Scheme 1, but the S11 molecule returns from excited structure of ICT to the ground state due to unavailability of the resonance structure shown in the case of S10. The spectral results showed that the presence of the ICT and TICT process that occurs upon photo-excitation is not only solvent polarity but also the hydrogen bond ability of strong hydrogen bond acceptors such as DMF and DMSO.^{29,32}

We have determined the solvent-solute interactions with multiple linear regression analysis. According to the Kamlet-Taft regression results, the coefficients of π^* and β are significantly higher than the coefficient of α . This indicated that the absorption and emission spectral shifts are controlled by polarity/dipolarizability of nonspecific interactions and hydrogen bond acceptor (HBA) ability.³³

3. Experimental

3.1. Equipment

The UV-Vis absorption and fluorescence spectra of the samples were recorded with a PerkinElmer Lambda 35 UV/VIS spectrophotometer and Shimadzu RF-5301PC spectrofluorophotometer, respectively. Fluorescence and absorption measurements were recorded for all sulfonamide derivatives at room temperature. For the steady-state fluorescence measurements, all samples were excited at 320 nm and fluorescence intensity was recorded between 330 nm and 550 nm. The fluorescence lifetime measurements were carried out with a LaserStrobe

model TM3 spectrofluorophotometer from Photon Technology International. The excitation source combined a pulsed nitrogen laser/tunable dye laser. The samples were excited at 366 nm. The decay curves were collected over 200 channels using a nonlinear time scale with the time increment increasing according to arithmetic progression. The fluorescence decays were analyzed with the lifetime distribution analysis software from the instrument supplying company. The quality of fits was assessed by χ^2 values and weighed residuals.³⁴

The fluorescence quantum yields of donor molecules were calculated through the Parker–Rees equation:

$$\Phi_s = \Phi_r \left(\frac{D_s}{D_r} \right) \left(\frac{n_s^2}{n_r^2} \right) \left[\frac{1 - 10^{-OD_r}}{1 - 10^{-OD_s}} \right], \quad (1)$$

where D is the integrated area under the corrected fluorescence spectrum, n is the refractive index of the solution, and OD is the optical density at the excitation wavelength ($\lambda_{ex} = 320$ nm). The subscripts s and r refer to the sample and reference solutions, respectively. Quinine sulfate in 0.5 M H_2SO_4 solution was used as the reference. The fluorescence quantum yield of quinine sulfate was 0.54 in 0.5 M H_2SO_4 solution.³⁵

The rate constants of the radiative (k_r) and nonradiative (k_{nr}) deactivation were calculated by using the following equations:³⁶

$$k_r = \frac{\Phi_f}{\tau_f} \quad (2)$$

$$\frac{1}{\tau_f} = k_r + k_{nr}, \quad (3)$$

where Φ_f is fluorescence quantum yield and τ_f is fluorescence lifetime of samples.

3.2. Chemicals

All solvents (Sigma and Merck), quinine sulfate (Fluka), and H_2SO_4 (Sigma) were purchased and used without further purification. The physical properties and polarity parameters of all solvents used in the study are listed in Table 5.^{8,24} The stock solution of all compounds was prepared in MeOH. A certain amount of fresh probe samples in different solutions was obtained from this stock solution by evaporating the solvent. For all measurements, the concentrations of compounds were 1.0×10^{-5} M. All the experiments were performed at room temperature.

3.3. Synthesis of compounds S10 and S11

Compounds S10 and S11 were synthesized as described in our previous study.²³ Scheme 2 summarizes the synthesis of the compounds briefly and their chemical structures.

3.4. Estimation of dipole moments

A solvatochromic method was used for the determination of the ground and excited state dipole moment of the molecules, based on linear correlation between the band maximum of absorption, fluorescence, and solvent polarity function. ν_a : absorption and ν_f : fluorescence band maxima (cm^{-1}), ϵ : dielectric constant and n : refractive index of solvent

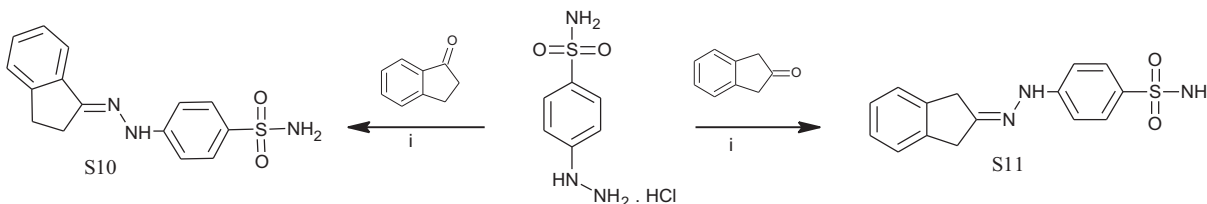
$$\tilde{\nu}_a - \tilde{\nu}_f = m_1 f(\epsilon, n) + const \quad (4)$$

$$\tilde{\nu}_a + \tilde{\nu}_f = -m_2 [f(\epsilon, n) + 2g(n)] + const, \quad (5)$$

Table 5. Physical properties, polarity functions, and Kamlet–Taft parameters of selected solvent.

Solvent	ϵ^a	η^b	$E_T(30)^c$	$E_T^{N(d)}$	$f(\epsilon, \eta)$	$g(\eta)$	α	β	π^*
Diethylether	4.3	1.353	34.5	0.117	0.370	0.851	0.00	0.47	0.24
1,4-Dioxane	2.2	1.422	36.0	0.164	0.044	0.617	0.00	0.37	0.49
Chloroform	4.8	1.445	39.1	0.259	0.371	0.975	0.20	0.10	0.69
DCM	8.9	1.424	40.7	0.309	0.590	1.166	0.13	0.10	0.73
THF	7.5	1.465	37.4	0.207	0.521	1.151	0.00	0.55	0.55
Ethyl acetate	6.1	1.372	38.1	0.228	0.493	0.999	0.00	0.45	0.45
DMF	36.7	1.430	43.2	0.386	0.836	1.419	0.00	0.69	0.88
DMSO	46.7	1.479	45.1	0.444	0.840	1.488	0.00	0.76	1.00
ACN	36.6	1.344	45.6	0.460	0.861	1.330	0.19	0.40	0.66
i-PrOH	20.2	1.377	48.4	0.546	0.781	1.294	0.76	0.84	0.48
n-Butanol	17.5	1.399	49.7	0.586	0.750	1.293	0.84	0.84	0.47
n-PrOH	20.8	1.384	50.7	0.617	0.783	1.305	0.84	0.90	0.52
EtOH	25.3	1.361	51.9	0.654	0.817	1.309	0.86	0.75	0.54
MeOH	33.0	1.329	55.4	0.762	0.855	1.304	0.98	0.66	0.60

^a Dielectric constant. ^b Refractive index. ^c Reichardt empirical polarity parameter. ^d Molecular-microscopic solvent polarity parameter. THF; tetrahydrofuran. DCM; dichloromethane. DMF; dimethylformamide. DMSO; dimethyl sulfoxide. ACN; acetonitrile. i-PrOH; iso-propanol. n-PrOH; n-propanol. EtOH; ethanol. MeOH; methanol i = Sodium acetate, ethanol, 60 min, 78 °C, 150 W

**Scheme 2.** Synthesis of compounds S10 and S11.

where

$$f(\epsilon, n) = \frac{2n^2 + 1}{n^2 + 2} \left[\frac{\epsilon - 1}{\epsilon + 2} - \frac{n^2 - 1}{n^2 + 2} \right] \quad (6)$$

$$g(n) = \frac{3}{2} \left[\frac{n^4 - 1}{(n^2 + 2)^2} \right] \quad (7)$$

and

$$m_1 = \frac{2(\mu_e - \mu_g)^2}{hca^3} \quad (8)$$

$$m_2 = \frac{2(\mu_e^2 - \mu_g^2)^2}{hca^3} \quad (9)$$

h is Planck's constant, c is the velocity of light in the vacuum, μ_g and μ_e are the dipole moments of solute in the ground and excited states, and a is Onsager cavity radius.^{30,37} Onsager cavity radius can be calculated

from the molecular volume of the molecule. Suppan's equation is used for the calculation of Onsager cavity radius.^{38,39}

$$a = \left(\frac{3M}{4\pi dN} \right)^{1/3}, \quad (10)$$

where d is the density (1.40 g/cm^3).⁴⁰ and M is the molecular weight of molecules, respectively. N is Avogadro's number. Onsager cavity radius values were calculated as 4.40 \AA using Eq. (10).

Considering parallel orientations for the molecular dipole moment in ground and excited states, based on Eqs. (8) and (9), the following equations are obtained:³⁷

$$\mu_g = \frac{m_2 - m_1}{2} \left[\frac{hca^3}{2m_1} \right]^{1/2} \quad (11)$$

$$\mu_e = \frac{m_2 + m_1}{2} \left[\frac{hca^3}{2m_1} \right]^{1/2} \quad (12)$$

Moreover, the changes in dipole moments ($\Delta\mu$) are determined with the solvatochromic method developed by Reichardt using microscopic solvent polarity parameter (E_T^N).⁴¹ According to the method,

$$\nu_a - \nu_f = 11307.6 \left[\left(\frac{\Delta\mu}{\Delta\mu_D} \right)^2 \left(\frac{a_D}{a} \right)^3 \right] E_T^N + \text{const}, \quad (13)$$

where $\Delta\mu_D$ is the change in the dipole moment of the betaine dye (9 D) and a_D is the Onsager cavity radius of betaine dye (6.2 \AA). The change in dipole moments was calculated by Eq. (14) using these values.

$$\Delta\mu = \left[\frac{81m}{(6.2/a)^3 11307.6} \right]^{1/2}, \quad (14)$$

where m is the slope of the linear plot of E_T^N vs. Stokes shift (Figure 5) and a is Onsager cavity radius.⁴²

To characterize the solvent-solute interactions, multiple linear regression analysis suggested by Kamlet-Taft was used. The multiple linear regression can be described by the following equation:

$$\Delta\nu = \Delta\nu_0 + a\alpha + b\beta + c\pi^*, \quad (15)$$

where ν_0 stands for the peak frequency of the solute in a gas phase. α , β , and π^* denote the hydrogen bond donor (HBD) ability, hydrogen bond acceptor (HBA) ability, and dipolarity/polarizability of the solvents respectively. a - c are the regression coefficients describing the sensitivity of the respective property to the different types of solvent-solute interactions. The Kamlet-Taft solvent parameters are listed in Table 5.

4. Conclusions

The newly synthesized sulfonamide derivatives were characterized in solvents having photophysically different polarities. The shifts in absorption and fluorescence spectra and the changes in the fluorescence quantum yield and lifetime values occurred depending on the solvent. For all solvents, it was observed that the fluorescence property of S11 is weaker and quantum yield of S11 is lower than S10. It was determined that both compounds

have higher quantum yield in the polar aprotic solvent. The ground and excited state dipole moments of compounds were also calculated using polarity functions and Stokes shifts. The results showed that for both compounds the excited state dipole moments are greater than those in ground state. The solvent polarity and specific solvent–solute interactions change the dipole moments of molecules upon transition from ground to excited state. Finally, determination of the photophysical properties and the dipole moments of these biologically active novel molecules is of great importance in many areas such as nonlinear optical devices, chemical sensing, and understanding the photochemical and photobiological processes.

References

1. Casey, K. G.; Quitevis, E. L. *J. Phys. Chem.* **1988**, *92*, 6590-6594.
2. Melavanki, R.; Patil, H. D.; Umamathy, S.; Kadadevarmath, J. S. *J. Fluoresc.* **2012**, *22*, 137-144.
3. Alty, I. G.; Cheek, D. W.; Chen, T.; Smith, D. B.; Walhout, E. Q.; Abelt, C. J. *J. Phys. Chem. A* **2016**, *120*, 3518-3523.
4. Bettaieb, L.; Aaron, J. J. *Turk. J. Chem.* **2001**, *25*, 165-171.
5. Rao, C. N. R.; Singh, S.; Senthilnathan, V. P. *Chem. Soc. Rev.* **1976**, *5*, 297-316.
6. Mallick, A.; Maiti, S.; Haldar, B.; Purkayastha, P.; Chattopadhyay, N. *Chem. Phys. Lett.* **2003**, *371*, 688-693.
7. Zakerhamidi, M. S.; Ghanadzadeh, A.; Moghadam, M. *Spectrochim. Acta, Part A* **2011**, *78*, 961-966.
8. Czerwińska, M.; Wierzbicka, M.; Guzow, K.; Bylińska, I.; Wiczak, W. *RSC Adv.* **2014**, *4*, 19310.
9. Acemioglu, B.; Arik, M.; Efeoğlu, H.; Onganer, Y. *J. Mol. Struct-Theochem.* **2001**, *548*, 165-171.
10. Oliveira, E.; Baptista, R. M. F.; Costa, S. P. G.; Raposo, M. M. M.; Lodeiro, C. *Photochem. Photobiol. Sci.* **2014**, *13*, 492-498.
11. Liu, L.; Sun, Y.; Wei, S.; Hu, X.; Zhao, Y.; Fan, J. *Spectrochim. Acta, Part A* **2012**, *86*, 120-123.
12. Guzow, K.; Szabelski, M.; Karolczak, J.; Wiczak, W. *J. Photochem. Photobiol., A* **2005**, *170*, 215-223.
13. Aggarwal, K.; Khurana, J. M. *Spectrochim. Acta, Part A* **2015**, *143*, 288-297.
14. Patil, N. R.; Melavanki, R. M.; Kapatkar, S. B.; Ayachit, N. H.; Saravanan, J. *J. Fluoresc.* **2011**, *21*, 1213-1222.
15. Peng, X.; Deng, J. G.; Xu, H. B. *RSC Adv.* **2013**, *3*, 24146.
16. Jiménez-Sánchez, A.; Rodríguez, M.; Métivier, R.; Ramos-Ortíz, G.; Maldonado, J. L.; Réboles, N.; Farfán, N.; Nakatani, K.; Santillan, R. *New J. Chem.* **2014**, *38*, 730-738.
17. Orłowski, R.; Banasiewicz, M.; Clermont, G.; Castet, F.; Nazir R.; Blanchard-Desce, M.; Gryko, D. T. *Phys. Chem. Chem. Phys.* **2015**, *17*, 23724-23731.
18. Gaber, M.; El-Daly, S. A.; Fayed, T. A.; El-Sayed, Y. S. *Opt. Laser Technol.* **2008**, *40*, 528-537.
19. Zhang, Y.; Jia, P.; Tong, Z.; Liu, H. B.; Wang, J. *Turk. J. Chem.* **2015**, *39*, 905-916.
20. Öter, Ö.; Aydın, M.; Ertekin, K. *Turk. J. Chem.* **2016**, *40*, 373-384.
21. Xu, H.; Wang, R.; Fan, C.; Liu, G.; Pu, S. *Turk. J. Chem.* **2016**, *40*, 38-53.
22. Asiri, A. M.; Alamry, K. A.; Pannipara, M.; Al-Sehemi, A. G.; El-Daly, S. A. *Spectrochim. Acta, Part A* **2015**, *149*, 722-730.
23. Gul, H. I.; Kucukoglu, K.; Yamali, C.; Bilginer, S.; Yuca, H.; Ozturk, I.; Taslimi, P.; Gulcin, I.; Supuran, C. T. *J. Enzyme Inhib. Med. Chem.* **2016**, *31*, 568-573.
24. Zakerhamidi, M. S.; Ahmadi-Kandjani, S.; Moghadam, M.; Ortyl, E.; Kucharski, S. *Spectrochim. Acta, Part A* **2012**, *85*, 105-110.
25. Kucherak, O. A.; Richert, L.; Mely, Y.; Klymchenko, A. S. *Phys. Chem. Chem. Phys.* **2012**, *14*, 2292-2300.
26. Jones, G.; Jackson, W. R.; Choi, C. Y.; Bergmark, W. R. *J. Phys. Chem.* **1985**, *89*, 294-300.

27. Grabowski, Z. R.; Rotkiewicz, K.; Rettig, W. *Chem. Rev.* **2003**, *103*, 3899-4032.
28. Nad, S.; Pal, H. *J. Phys. Chem. A* **2001**, *105*, 1097-1106.
29. Benazzouz, A.; Makhloufi-Chebli, M.; Hamdi, S. M.; Boutemour-Kheddis, B.; Silva, A. M. S.; Hamdi, M. *J. Mol. Liq.* **2016**, *219*, 173-179.
30. Patil, S. K.; Wari, M. N.; Panicker, C. Y.; Inamdar, S. R. *Spectrochim. Acta, Part A* **2014**, *123*, 117-126.
31. Reichardt, C. *Solvents and Solvent Effects in Organic Chemistry*. Wiley-VCH: Weinheim, Germany, 2004.
32. Joshi, S.; Kumari, S.; Bhattacharjee, R.; Sakhuja, R.; Pant, D. D. *J. Mol. Liq.* **2015**, *209*, 219-223.
33. Alphonse, R.; Varghese, A.; George, L.; Nizam, A. *J. Mol. Liq.* **2016**, *215*, 387-395.
34. Bozkurt, E.; Acar, M.; Onganer, Y.; Meral, K. *Phys. Chem. Chem. Phys.* **2014**, *16*, 18276-18281.
35. Tan, A.; Bozkurt, E.; Kishali, N.; Kara, Y. *Helv. Chim. Acta* **2014**, *97*, 1107-1114.
36. Valeur, B. *Molecular Fluorescence - Principles and Applications*. Wiley-VCH: Weinheim, Germany, 2001.
37. Kabatc, J.; Ośmiałowski, B.; Pączkowski, J. *Spectrochim. Acta, Part A* **2006**, *63*, 524-531.
38. Lopez-de-Luzuriaga, J. M.; Manso, E.; Monge, M.; Olmos, M. E.; Rodriguez-Castillo, Sampedro, M.; D. *Dalton Trans.* **2015**, *44*, 11029-11039.
39. Basavaraja, J.; Inamdar, S. R.; Suresh Kumar, H. M. *Spectrochim. Acta, Part A* **2015**, *137*, 527-534.
40. A. C. D. S. V11.02 ACD/Labs, 1994-2015.
41. Reichardt, C. *Chem. Rev.* **1994**, *94*, 2319-2358.
42. Ravi, M.; Soujanya, T.; Samanta, A.; Radhakrishnan, T. P. *J. Chem. Soc., Faraday Trans.* **1995**, *91*, 2739-2742.